

- [1] R. Robson, *J. Chem. Soc. Dalton Trans.* **2000**, 3735; b) S. R. Batten, *CrystEngComm* **2001**, 18; c) O. M. Yaghi, H. Li, C. Davis, D. Richardson, T. L. Groy, *Acc. Chem. Res.* **1998**, *31*, 474; d) S. Kitagawa, M. Kondo, *Bull. Chem. Soc. Jpn.* **1998**, *71*, 1739; e) D.-L. Long, A. J. Blake, N. R. Champness, C. Wilson, M. Schröder, *Angew. Chem.* **2001**, *113*, 2509; *Angew. Chem. Int. Ed.* **2001**, *40*, 2443; f) S. A. Bourne, J. Lu, A. Mondal, B. Moulton, M. J. Zaworotko, *Angew. Chem.* **2001**, *113*, 2169; *Angew. Chem. Int. Ed.* **2001**, *40*, 2111.
- [2] H. Li, M. Eddaoudi, M. O'Keeffe, O. M. Yaghi, *Nature* **1999**, *402*, 276; b) S. S.-Y. Chui, S. M.-F. Lo, J. P. H. Charmant, A. G. Orpen, I. D. Williams, *Science* **1999**, *283*, 1148; c) S.-I. Noro, S. Kitagawa, M. Kondo, K. Seki, *Angew. Chem.* **2000**, *112*, 2161; *Angew. Chem. Int. Ed.* **2000**, *39*, 2081; d) J.-S. Seo, D. Whang, H. Lee, S. I. Jun, J. Oh, Y. J. Jeon, K. Kim, *Nature* **2000**, *404*, 982; e) B. F. Abrahams, P. A. Jackson, R. Robson, *Angew. Chem.* **1998**, *110*, 2801; *Angew. Chem. Int. Ed.* **1998**, *37*, 2656; f) C. J. Kepert, M. J. Rosseinsky, *Chem. Commun.* **1999**, 375; g) A. J. Fletcher, E. J. Cussen, T. J. Prior, M. J. Rosseinsky, C. J. Kepert, K. M. Thomas, *J. Am. Chem. Soc.* **2001**, *123*, 10001.
- [3] M. Fujita, Y. J. Kwon, S. Washizu, K. Ogura, *J. Am. Chem. Soc.* **1994**, *116*, 1151; b) R. W. Gable, B. F. Hoskins, R. Robson, *J. Chem. Soc. Chem. Commun.* **1990**, 1677; c) M. J. Zaworotko, *Chem. Commun.* **2001**, 1.
- [4] To date only six coordination complexes (see reference [6]) were reported using **1**, whereas there are more than 100 structures reported using 4,4'-bipyridine.
- [5] M. Fujita, K. Umemoto, M. Yoshizawa, N. Fujita, T. Kusukawa, K. Biradha, *Chem. Commun.* **2001**, 509–518.
- [6] S. R. Batten, B. F. Hoskins, R. Robson, *J. Am. Chem. Soc.* **1995**, *117*, 5385; b) S. R. Batten, B. F. Hoskins, R. Robson, *Angew. Chem.* **1995**, *107*, 884; *Angew. Chem. Int. Ed. Engl.* **1995**, *34*, 820; c) B. F. Abrahams, S. R. Batten, H. Hamit, B. F. Hoskins, R. Robson, *Angew. Chem.* **1996**, *108*, 1794; *Angew. Chem. Int. Ed. Engl.* **1996**, *35*, 1690; d) B. F. Abrahams, S. R. Batten, H. Hamit, B. F. Hoskins, R. Robson, *Chem. Commun.* **1996**, 1313; e) B. F. Abrahams, S. R. Batten, M. J. Grannas, H. Hamit, B. F. Hoskins, R. Robson, *Angew. Chem.* **1999**, *111*, 1538; *Angew. Chem. Int. Ed.* **1999**, *38*, 1475; f) S. R. Batten, B. F. Hoskins, B. Moubarak, K. S. Murray, R. Robson, *Chem. Commun.* **2000**, 1095.
- [7] Examples of dynamic coordination networks: a) R. Kitaura, K. Fujimoto, S.-i. Noro, M. Kondo, S. Kitagawa, *Angew. Chem.* **2002**, *114*, 149; *Angew. Chem. Int. Ed.* **2002**, *41*, 141; b) L. C. Tabares, J. A. R. Navarro, J. M. Salas, *J. Am. Chem. Soc.* **2001**, *123*, 383; c) D. V. Soldatov, J. A. Ripmeester, S. I. Shergina, I. E. Sokolov, A. S. Zanina, S. A. Gromilov, Y. A. Dyadin, *J. Am. Chem. Soc.* **1999**, *121*, 4179; d) G. Alberti, S. Murcia-Mascarós, R. Vivani, *J. Am. Chem. Soc.* **1998**, *120*, 9291; e) K. S. Min, M. P. Suh, *J. Am. Chem. Soc.* **2000**, *122*, 6384.
- [8] S. R. Batten, R. Robson, *Angew. Chem.* **1998**, *110*, 1558; *Angew. Chem. Int. Ed.* **1998**, *37*, 1460.
- [9] Some interpenetrated networks with a (10,3)-b configuration: a) G. B. Gardner, Y.-H. Kiang, S. Lee, A. Asgaonkar, D. Venkatraman, *J. Am. Chem. Soc.* **1996**, *118*, 6947; b) L. Carlucci, G. Ciani, D. M. Proserpio, A. Sironi, *J. Am. Chem. Soc.* **1995**, *117*, 4562; c) F. A. Cotton, C. Lin, C. A. Murillo, *J. Chem. Soc. Dalton Trans.* **2001**, 499; d) O. M. Yaghi, H. Li, *J. Am. Chem. Soc.* **1995**, *117*, 10401.
- [10] Crystal data for **2**: Monoclinic, *C2/c*, *a* = 36.079(10), *b* = 14.978(4), *c* = 30.734(9) Å, β = 102.470(2)°, *V* = 16217(12) Å³, *Z* = 8, *D_c* = 1.851 g cm⁻³, 9066 reflections out of 14243 unique reflections with *I* > 2σ(*I*), 1.16 < θ < 25.00°, final *R* factors *R₁* = 0.079, *wR₂* = 0.2316.
- [11] Crystal data for **3**: Monoclinic, *C2/c*, *a* = 35.487(8), *b* = 15.080(4), *c* = 31.542(7) Å, β = 102.107(4)°, *V* = 16504(7) Å³, *Z* = 8, *D_c* = 1.772 g cm⁻³, 9884 reflections out of 14518 unique reflections with *I* > 2σ(*I*), 1.32 < θ < 25.00°, final *R* factors *R₁* = 0.0638, *wR₂* = 0.1922.
- [12] Crystal data for **2'**: Triclinic, *P1̄*, *a* = 14.297(3), *b* = 17.164(3), *c* = 27.333(5) Å, α = 89.970(5)°, β = 77.104(4)°, γ = 74.591(4)°, *V* = 6291(2) Å³, *Z* = 4, 6564 reflections out of 21852 unique reflections with *I* > 2σ(*I*), 1.16 < θ < 25.00°, final *R* factors *R₁* = 0.1194, *wR₂* = 0.2720.
- [13] Crystal data for **3'**: Monoclinic, *C2/c*, *a* = 27.482(8), *b* = 15.096(4), *c* = 31.846(7) Å, β = 94.143(6)°, *V* = 13177(6) Å³, *Z* = 8, 8052 reflections out of 11604 unique reflections with *I* > 2σ(*I*), 1.28 < θ < 25.00°, final *R* factors *R₁* = 0.0623, *wR₂* = 0.1462.
- [14] Crystals of **2'** placed in nitrobenzene: The crystals broke into small pieces, monoclinic, *C2/c*, *a* = 36.370(7), *b* = 15.090(3), *c* = 31.266(6) Å, β = 103.782(4)°, *V* = 16665(5) Å³, *Z* = 8, 5583 reflections out of 14665 unique reflections with *I* > 2σ(*I*), 1.15 < θ < 25.00°, final *R* factors *R₁* = 0.0994, *wR₂* = 0.2486.
- [15] Unit cell parameters for **2** after complete guest removal by heating on hotplate for 10 mins at 170 °C, the crystals broke into small pieces and became less transparent. The complete guest removal was confirmed by GC analysis: *a* = 14.573(19), *b* = 17.268(23), *c* = 28.044(38) Å, α = 89.685(15)°, β = 76.956(14)°, γ = 73.794(12)°. Heating the crystals of **3** to 170 °C resulted in similar cell parameters to those described above.
- [16] The powder diffraction patterns for **2** monitored at various time intervals are in the Supporting Information.
- [17] Crystal data for **4**: Monoclinic, *C2/c*, *a* = 35.316(3), *b* = 14.7247(14), *c* = 31.766(3) Å, β = 101.906(2)°, *V* = 16163(7) Å³, *Z* = 8, *D_c* = 1.686 g cm⁻³, 10419 reflections out of 14232 unique reflections with *I* > 2σ(*I*), 1.50 < θ < 25.00°, final *R* factors *R₁* = 0.0557, *wR₂* = 0.1589.
- [18] Crystal data for **5**: Orthorhombic, *Fdd2*, *a* = 35.252(5), *b* = 39.509(5), *c* = 8.153(1) Å, *V* = 11355(3) Å³, *Z* = 8, *D_c* = 2.442 g cm⁻³, 3752 reflections out of 4976 unique reflections with *I* > 2σ(*I*), 1.55 < θ < 24.99°, final *R* factors *R₁* = 0.0456, *wR₂* = 0.1038.

Crystal-to-Crystal Sliding of 2D Coordination Layers Triggered by Guest Exchange**

Kumar Biradha, Yoshito Hongo, and Makoto Fujita*


Metal-organic frameworks containing channels or voids have attracted current interest because of their functional properties, which are similar to those of zeolites and clays.^[1–4] Although the porosity is one of the most studied properties of metal-organic frameworks, there are very few studies on dynamic porous coordination networks.^[5] 2D-network materials have the potential to provide such dynamic porous materials as they can adopt changes caused by external stimuli, either within the layer or in between the layers. Here we present one such unique and novel dynamic process in the crystals of a 2D net containing square grids of dimension 20 × 20 Å.

The crystal-to-crystal sliding of the 2D nets between two packing modes A and B (Figure 1) is triggered by guest exchange, and results in considerable increase in the dimensions of channels. This crystal-to-crystal transformation was evidenced by single crystal and powder X-ray diffraction studies before and after the transformation. The single-crystal

[*] Prof. Dr. M. Fujita,[†] Dr. K. Biradha, Y. Hongo
Department of Applied Chemistry
Graduate School of Engineering, Nagoya University
and
CREST, Japan Science and Technology Corporation (JST)
Chikusaku, Nagoya 464-8603 (Japan)
E-mail: mfujita@appchem.t.u-tokyo.ac.jp

[†] Present address:
The University of Tokyo Bunkyo-ku, Tokyo 113-8656 (Japan)
Fax: (+81)3-5841-7257

[**] This work was supported in part by the Grant-In-Aid for Science Research in a Priority Area "Metal-Assembled Complexes (no. 401-10149106) from the Ministry of Education, Science, Sports, and Culture, Japan.

 Supporting information for this article is available on the WWW under <http://www.angewandte.org> or from the author.

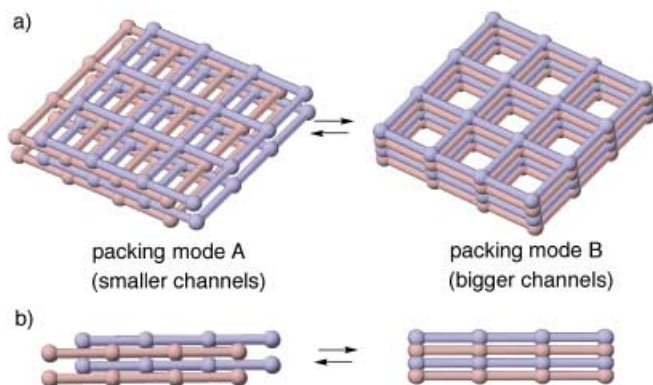


Figure 1. Schematic representation of the sliding of 2D square grids: a) top and b) side views. Channels across the layers are smaller in mode A than in mode B.

analysis of unit cell parameters at various time intervals during the transformation suggested that the first step is the exchange of guest molecules and the second step is the sliding of the layers. Furthermore, the guest-exchanged crystal with larger channel dimensions (packing mode B) is found to absorb/desorb guest molecules, while such a property is lacking in their parent crystals (packing mode A).

We have recently shown that the long ligand, 4,4'-bis(4-pyridyl)biphenyl (**1**), forms $[\text{Ni}(\text{1})_2(\text{NO}_3)_2 \cdot 4(o\text{-xylene})]$ (**2**) upon reaction with $\text{Ni}(\text{NO}_3)_2$ in the presence of *o*-xylene.^[4] Complex **2** contains 2D layers that are formed by square grids of dimension $20 \times 20 \text{ \AA}$.^[6] These layers have a short interlayer separation of 4.1 \AA and can slide on each other as the binding forces between the layers are only weak aromatic and $\text{C}\cdots\text{H}\cdots\text{O}$ interactions that are reformed after the sliding is completed.^[7]

Interestingly, the crystals of **2** show a remarkable ability to exchange the guest molecule *o*-xylene for mesitylene but not for *m*-xylene, or 1,3- or 1,2-dimethoxybenzene. In a typical reaction, the crystals of **2** were immersed in mesitylene for 6 h and then the absorbed guest was extracted into diethyl ether following addition of HCl to the dried crystals. The GC analysis of the extracted layer showed only the presence of mesitylene, which indicates the complete exchange of the *o*-xylene guest. The chemical composition of the crystals in which the *o*-xylene guest had been replaced with mesitylene was $[\text{Ni}(\text{1})_2(\text{NO}_3)_2 \cdot 1.7(\text{mesitylene})]_n$ from elemental analysis. Notably the crystalline nature was not destroyed during the process and hence crystals suitable for an X-ray analysis were obtained even after the guest exchange.

Surprisingly, the single-crystal X-ray analysis of the crystals with mesitylene as the new guest (**3**) revealed that considerable sliding of the layers on each other occurred such that the dimension of the channels was bigger than that of **2** (Figure 2). For example, the nearest distance between Ni atoms of the adjacent layers in **2** is 11.46 \AA whereas it is 8.06 \AA in **3**. Assuming that one of the layers is fixed, the approximate sliding distance of its neighboring layer can be calculated as 4.2 \AA , based on the geometry of the Ni atoms. In **2** the layers pack on each other such that they overlap in one direction and are offset in the other direction, which results in the approximate channel dimension of about $10 \times 20 \text{ \AA}$ (packing

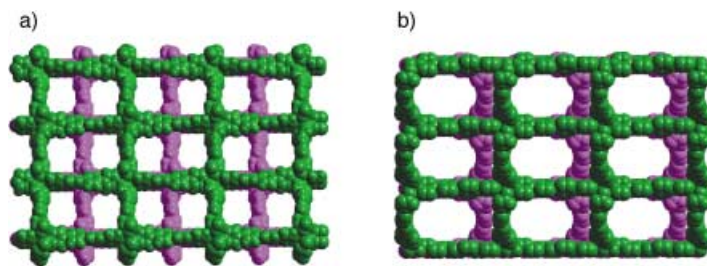


Figure 2. Packing of 2D layers in a) **2** (mode A) and b) **3** (mode B). Alternate layers colored in magenta and green. Notice the differences in channel dimensions.

mode A). Unlike **2**, the offset packing was not observed in **3** as the layers slide on each other to give channel dimensions of approximately $15 \times 20 \text{ \AA}$ (packing mode B).

In both packing motifs, edge-to-face aromatic interactions exist at the corner of the channels but not along the walls—the shortest centroid-to-centroid distances of the C_6 rings of **1** in the neighboring layers are 4.869 and 4.819 \AA for A and B, respectively. There are more $\text{C}\cdots\text{H}\cdots\text{O}$ hydrogen bonds between the nitrate ions and phenyl groups of adjacent layers in mode B (six) than mode A (three). This disparity is because in mode A only one of the C_6 rings of **1** participate in $\text{C}\cdots\text{H}\cdots\text{O}$ hydrogen bonds whereas in mode B both of the C_6 rings participate. The entire framework of **3**, except one of the phenylene rings of **1**, had no disorder though the mesitylene molecules were highly disordered. The electron density peaks corresponding to the disordered mesitylene were distributed throughout the channels. Analysis of the structure in detail showed that the grids in **3** are somewhat contracted compared to those in **2**: $19.79 \times 19.96 \text{ \AA}$ in **3** and $19.91 \times 19.96 \text{ \AA}$ in **2** (Figure 3). Furthermore, the unit-cell volume of **3** is 7% less than that of **2**.

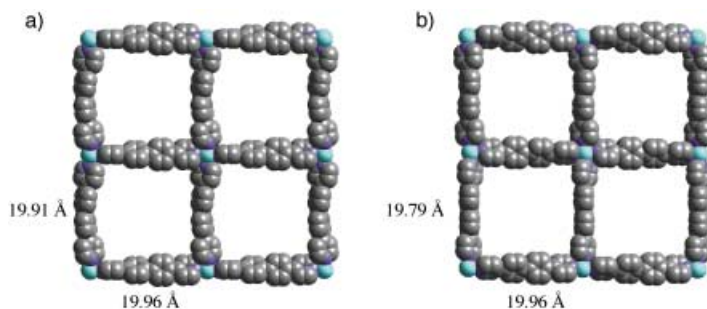


Figure 3. 2D square grid layers exhibited in a) **2** and b) **3**. The disorder in one of the C_6 rings of ligand **1** in the crystals of **3** is not shown.

The sliding of the 2D net was also monitored by X-ray powder diffraction pattern (XRPD) of the crystals. The conversion of crystal **2** into **3** by the guest exchange resulted in considerable change in the diffraction pattern. Further, the reexchange of mesitylene in **3** with *o*-xylene suggested that mode A was regenerated in a high percentage (see Supporting Information).^[8]

To establish the mechanism for guest exchange and sliding of the layers, the reaction was monitored over time by single crystal diffraction, that is, the unit-cell parameters were

determined at various time intervals, with the crystal of **2** in a glass capillary filled with mesitylene. Interestingly the results indicate no change in cell parameters (similar to **2**) up to 6 h, which is the time required for exchange of guest molecules as indicated by GC analysis. From 6 h to 9 h the crystal was not indexed but still showed diffraction. At 10 h the indexing was restarted to give cell parameters similar to those of **3**. The crystal was monitored again at 22 h and it was indexed with more reflections than at 10 h, which gave cell parameters similar to those of **3**. These results clearly indicate that the transformation indeed occurred crystal to crystal; the first step is guest exchange and the second step is the sliding of the layers.

The changes in terms of single crystal diffraction were illustrated in one of the frames recorded at various time intervals (Figure 4). Up to 3.5 h the diffraction pattern was constant but from 3.5 h the pattern changed slowly. The spots

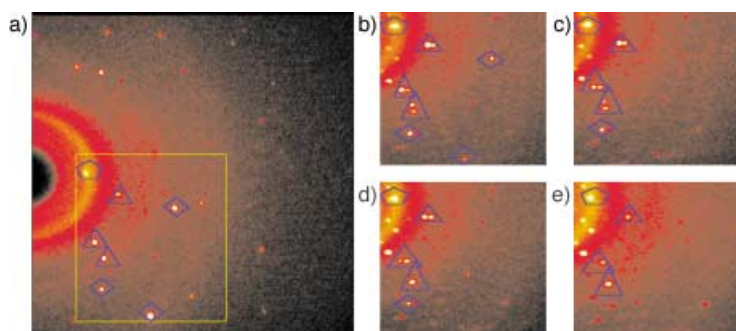


Figure 4. Diffraction patterns for transformation at various time intervals after immersion of crystal of **2** in mesitylene: a) The full frame after 15 mins. The region shown in a square box in a) after b) 4.30 h; c) 6 h; d) 8 h; e) 10 h. For comparison, the spots are marked with polygons (see text).

shown in diamonds disappeared and those shown in triangles divided into two and finally merged. The spot shown in a pentagon intensified as the time progressed and its position remained constant throughout the reaction. Some new peaks also appeared as the time progressed.

The role of mesitylene seems to be important in this transformation as a similar transformation or guest exchange was not observed when the crystals of **2** were immersed for even longer in the other guest solvents such as benzene, *m*-xylene, or 1,2- or 1,3-dimethoxybenzene. In the hope of growing crystals of **3** directly, the complexation of ligand **1** with $\text{Ni}(\text{NO}_3)_2$ was carried out in the presence of mesitylene. However this reaction resulted in fourfold, perpendicularly interpenetrated square-grid networks instead of an open framework structure.^[9]

Unlike **2**, which exhibited selectivity in guest exchange, **3** can exchange mesitylene for many liquid aromatic guest molecules without destroying or altering the crystal nature.^[10] The unit-cell parameters after the exchange of mesitylene with guests such as nitrobenzene and *o*-xylene were found to be the same as those of **3**. Guest absorption reactions were carried out on **3** after removing the mesitylene by heating it to 100 °C at 5 mmHg for 6 h. The crystals from which the

mesitylene was removed were also in packing mode B. Interestingly, the immersion of these crystals in aromatic guest solvents lead to absorption of the guests while retaining their crystalline nature; this was verified by GC, elemental analysis, and XRPD.^[11]

Experimental Section

Synthesis of 3: The crystals of **2** were immersed in mesitylene for a day and then the complete exchange of *o*-xylene for mesitylene was verified by GC analysis. The unit-cell parameters for some of these crystals were measured with single crystal diffraction and all of them were found to have similar cell parameters to those of **3**.

Elemental analysis: **2:** $[(\text{Ni}(\text{I})_2(\text{NO}_3)_2) \cdot 3.5(\text{o-xylene})]$, 0.5 equivalents of guest escaped at RT: calcd (%) C 73.85, H 5.77, N 7.18; found C 73.53, H 5.72, N 7.11; **3:** $[(\text{Ni}(\text{I})_2(\text{NO}_3)_2) \cdot 1.7(\text{mesitylene})]$: calcd (%) C 70.96, H 5.26, N 8.37; found C 70.50, H 5.25, N 8.37.

Crystal data for 2: Monoclinic, $C2/c$, $a = 27.187(3)$, $b = 19.963(2)$, $c = 12.685(4)$ Å, $\beta = 106.923(2)^\circ$, $V = 6585.9(12)$ Å³, $Z = 4$, $D_c = 1.235$ g cm⁻³, 5932 unique reflections out of 7770 with $I > 2\sigma$, $1.29 < \theta < 27.98^\circ$, final R factors $R_1 = 0.067$, $wR_2 = 0.205$. **Crystal data for 3:** Monoclinic, $P2_1/c$, $a = 13.071(3)$, $b = 19.853(4)$, $c = 12.082(3)$ Å, $\beta = 103.149(4)^\circ$, $V = 3053.1(11)$ Å³, $Z = 2$, 4527 unique reflections out of 7099 with $I > 2\sigma$, $1.90 < \theta < 27.94^\circ$, final R factors $R_1 = 0.087$, $wR_2 = 0.2219$. One of the C_6 rings of **1** was disordered; this was modeled and refined. Also the peaks corresponding to mesitylene were located and refined isotropically. The data for both **2** and **3** for were measured on a Siemens SMART/CCD diffractometer ($\text{MoK}\alpha$ radiation $\lambda = 0.71073$ Å) at 193 K. An empirical absorption correction was applied using SADABS program. Non-hydrogen atoms were refined anisotropically and hydrogen atoms were fixed at calculated positions and refined using a riding model. CCDC-141218 (**2**), and CCDC-187955 (**3**) contain the supplementary crystallographic data for this paper. These data can be obtained free of charge via www.ccdc.cam.ac.uk/conts/retrieving.html (or from the Cambridge Crystallographic Data Centre, 12, Union Road, Cambridge CB21EZ, UK; fax: (+44) 1223-336-0033; or deposit@ccdc.cam.ac.uk).

Received: March 5, 2002 [Z18832]

- [1] a) B. Chen, M. Eddaoudi, S. T. Hyde, M. O'Keffe, O. M. Yaghi, *Science* **2001**, 291, 1021; b) J. Lu, A. Mondal, B. Moulton, M. J. Zaworotko, *Angew. Chem.* **2001**, 113, 2171; *Angew. Chem. Int. Ed.* **2001**, 40, 2113; c) S.-I. Noro, S. Kitagawa, M. Kondo, K. Seki, *Angew. Chem.* **2000**, 112, 2161; *Angew. Chem. Int. Ed.* **2000**, 39, 2081; d) J.-S. Seo, D. Whang, H. Lee, S. I. Jun, J. Oh, Y. J. Jeon, K. Kim, *Nature* **2000**, 404, 982; e) M. Eddaoudi, H. Li, O. M. Yaghi, *J. Am. Chem. Soc.* **2000**, 122, 1391; f) S. S.-Y. Chui, S. M.-F. Lo, J. P. H. Charmant, A. G. Orphen, I. D. Williams, *Science* **1999**, 283, 1148; g) D. M. L. Goodgame, D. A. Grachvogel, D. J. Williams, *Angew. Chem.* **1999**, 111, 217; *Angew. Chem. Int. Ed.* **1999**, 38, 153.
- [2] a) S. R. Batten, R. Robson, *Angew. Chem.* **1998**, 110, 1558; *Angew. Chem. Int. Ed.* **1998**, 37, 1460; b) M. J. Zaworotko, *Chem. Commun.* **2001**, 1; c) O. M. Yaghi, H. Li, C. Davis, D. Richardson, T. L. Groy, *Acc. Chem. Res.* **1998**, 31, 474; d) S. Kitagawa, M. Kondo, *Bull. Chem. Soc. Jpn.* **1998**, 71, 1739; e) M. Fujita, Y. J. Kwon, S. Washizu, K. Ogura, *J. Am. Chem. Soc.* **1994**, 116, 1151.
- [3] a) M. Kondo, T. Okubo, A. Asami, S.-I. Noro, T. Yoshitomi, S. Kitagawa, T. Ishii, H. Matsuzaka, K. Seki, *Angew. Chem. Int. Ed.* **1999**, 111, 190; *Angew. Chem. Int. Ed.* **1999**, 38, 140; b) H. Li, M. Eddaoudi, T. L. Groy, O. M. Yaghi, *J. Am. Chem. Soc.* **1998**, 120, 8571.
- [4] K. Biradha, Y. Hongo, M. Fujita, *Angew. Chem. Int. Ed.* **2000**, 112, 4001; *Angew. Chem. Int. Ed.* **2000**, 39, 3843.
- [5] a) R. Kitaura, K. Fujimoto, S.-i. Noro, M. Kondo, S. Kitagawa, *Angew. Chem.* **2002**, 114, 149; *Angew. Chem. Int. Ed.* **2002**, 41, 141; b) L. C. Tabares, J. A. R. Navarro, J. M. Salas, *J. Am. Chem. Soc.* **2001**, 123, 383; c) D. V. Soldatov, J. A. Ripmeester, S. I. Shergina, I. E. Sokolov, A. S. Zanina, S. A. Gromilov, Y. A. Dyadin, *J. Am. Chem. Soc.* **1999**, 121, 4179; d) G. Alberti, S. Murcia-Mascarós, R. Vivani, *J. Am. Chem. Soc.* **1998**, 120, 9291; e) K. S. Min, M. P. Suh, *J. Am. Chem. Soc.* **2000**, 122, 6384.

- [6] The dimensions of the grid are defined as the distances between the metal atoms separated by **1**.
- [7] The interlayer separation is defined as the distance of the Ni atoms to the plane of the neighboring layer.
- [8] The diffraction pattern of **3** does not exactly match with the pattern that is calculated from its single-crystal data. This mismatch in X-ray powder diffraction patterns could be caused by incomplete conversion from mode A into mode B and hence **3** may also contain some impurity in the form of mode A packing.
- [9] Crystallographic information for interpenetrated network: This structure was solved in two space groups: $I41/a$, $a = b = 19.276(3)$; $c = 28.942(9)$ Å; $\alpha = \beta = \gamma = 90^\circ$ and $C2/c$, $a = 27.257(5)$; $b = 28.942(9)$; $c = 19.275(4)$ Å; $\beta = 134.992(4)^\circ$. The solvent molecules are highly disordered.
- [10] Styrene, nitrobenzene, and cyanobenzene were also found to exchange *o*-xylene in **2** in the same way as mesitylene.
- [11] Preliminary results on **3**, from which the mesitylene was removed, indicate that it shows sorption properties with gaseous benzene.

Amplified DNA Detection by Electrogenenerated Biochemiluminescence and by the Catalyzed Precipitation of an Insoluble Product on Electrodes in the Presence of the Doxorubicin Intercalator**

Fernando Patolsky, Eugenii Katz, and Itamar Willner*

The amplified sensing of nucleic acids on surfaces attracts research efforts directed to the development of DNA chips for gene analysis, the detection of genetic disorders, tissue matching, forensic applications, and molecular computation.^[1,2] Amplified electrochemical DNA detection was reported by the labeling of nucleic acids with a redox enzyme and amplifying the formation of the double-stranded system on the electrode surface by the activation of a secondary bioelectrocatalyzed process.^[3] A further approach involves the generation, on the electrode surface, of a redox-active replica for the analyzed DNA by using polymerase, and the application of the redox replica as a mediator for the activation of bioelectrocatalyzed transformations.^[4] A different approach for the amplified detection of DNA includes the labeling of the analyzed DNA, for example, with a biotin label, that allows the secondary association of an enzyme conjugate (e.g. avidin–alkaline phosphatase or avidin–horseradish peroxidase) that stimulates the biocatalyzed precipita-

tion of an insoluble product on the electrodes.^[5,6] Faradaic impedance spectroscopy, which probes the interfacial electron-transfer resistance at the electrode supports, or microgravimetric quartz-crystal-microbalance (QCM) measurements were used as transduction methods for the accumulation of the insoluble products on the respective surfaces, as a result of the primary DNA-recognition events. Alternative methods to amplify DNA-recognition processes include the use of particulate labels, such as liposomes,^[7] Au nanoparticles,^[8] or CdS nanoparticles^[9] as amplifying agents, and the electrochemical, microgravimetric QCM assay, and photoelectrochemical transduction of the DNA detection.

Electrogenenerated chemiluminescence is a rapidly progressing method to image biosensing events on surfaces.^[10,11] Studies pioneered by Bard and colleagues have employed Ru^{II}–polypyridine complexes that bind to a double-stranded (ds) DNA for the electroluminescent imaging of DNA on electrode surfaces.^[12] However, the partial binding of [Ru(bpy)₃]²⁺ (bpy = 2,2'-bipyridine) complexes to single-stranded DNA introduces significant background electroluminescence that prohibits the detection of low hybridization yields of DNA. The covalent labeling of nucleic acids with a Ru^{II}–trisbipyridine complex has been suggested as a possible route to resolve this difficulty.^[13] Herein we report two alternative methods for the amplified detection of DNA by using the doxorubicin intercalator as a dsDNA surface-confined label for the electrogeneration of H₂O₂. The generated H₂O₂ is then used to image the DNA by: 1) stimulated biochemiluminescence, and 2) stimulated biocatalyzed precipitation of an insoluble product on electrodes.

Figure 1 depicts the configuration of the DNA detection system. The thiolated nucleic acid **1** is assembled on an Au-electrode and the surface coverage derived from the microgravimetric (QCM) analysis^[7c] is 2×10^{-11} mol cm⁻². Then the **1**-functionalized gold surface is treated with 1-mercaptohexanol to block pinholes in the DNA-monolayer assembly associated with the electrode. The resulting monolayer-functionalized electrode is then treated with the complementary analyte-DNA **2**, to yield the dsDNA assembly on the electrode surface. The resulting system is further treated with doxorubicin (**3**), which is a specific intercalator in double-stranded CG base-pair-containing DNA sequences.^[14] The intercalator-stimulated amplified analysis of the nucleic acid **2** is outlined in Figure 2. Electrochemical reduction of the intercalated **3** leads to the electrocatalyzed reduction of O₂ to H₂O₂. The electrogenerated H₂O₂ in the presence of luminol and horseradish peroxidase (HRP) leads to the formation of 3-aminophthalate and biochemiluminescence ($\lambda = 425$ nm)^[10] which indicates the DNA hybridization process (Figure 2A). Alternatively, the electrogenerated H₂O₂ mediates in the presence of HRP the oxidation of 4-chloronaphthol (**4**) to the insoluble product **5**, which precipitates on the electrode.^[15] Precipitation of **5** on the electrode insulates the electrode surface and increases its interfacial electron-transfer resistance. The changes in the interfacial electron-transfer resistances can then be followed in the presence of an electrolyte-soluble redox probe, by using Faradaic impedance spectroscopy. The stimulated light emission, or the biocatalyzed precipitation of **5** occurs only if the dsDNA structure with the

[*] Prof. I. Willner, F. Patolsky, Dr. E. Katz
Institute of Chemistry
The Farkas Center for Light-Induced Processes
The Hebrew University of Jerusalem
Jerusalem 91904 (Israel)
Fax: (+972) 2-6527715
E-mail: willner@vms.huji.ac.il

[**] This research is supported by the German–Israeli Program (DIP). The Max Planck Award for International Cooperation (I.W.) is gratefully acknowledged.

Supporting information for this article is available on the WWW under <http://www.angewandte.org> or from the author.